Bioorganic & Medicinal Chemistry 19 (2011) 6292–6301

Contents lists available at SciVerse ScienceDirect

Bioorganic & Medicinal Chemistry

journal homepage: www.elsevier.com/locate/bmc

Synthesis, molecular modeling and preliminary biological evaluation of a set of 3-acetyl-2,5-disubstituted-2,3-dihydro-1,3,4-oxadiazole as potential antibacterial, anti-*Trypanosoma cruzi* and antifungal agents

Marina Ishii *, Salomão Dória Jorge, Alex Alfredo de Oliveira, Fanny Palace-Berl, Ieda Yuriko Sonehara, Kerly Fernanda Mesquita Pasqualoto, Leoberto Costa Tavares

Department of Biochemical and Pharmaceutical Technology, Faculty of Pharmaceutical Sciences, University of São Paulo, Avenida Professor Lineu Prestes, 580, Bloco 16, Butantã, São Paulo, SP 05508-900, Brazil

ARTICLE INFO

Article history:
Received 21 June 2011
Revised 29 August 2011
Accepted 6 September 2011
Available online 10 September 2011

Keywords:
Oxadiazolines
Bacterial resistance
MRSA
VISA
Trypanosoma cruzi
Candida albicans

ABSTRACT

A series of 3-acetyl-2,5-disubstituted-2,3-dihydro-1,3,4-oxadiazole derivatives was synthesized and their activity screened in vitro against *Staphylococcus aureus*, *Trypanosoma cruzi*, and *Candida albicans*. The bioactivity was expressed as minimum inhibitory concentration (MIC) for *S. aureus* strains, and as fifty-percent inhibitory concentration (IC_{50}) of parasite population growth for *T. cruzi*. A molecular modeling approach was performed to establish qualitative relationships regarding the biological data and the compounds' physicochemical properties. The 5-(4-OC_4H_9Ph, **5l**), and 5-(4-CO_2CH_3Ph, **5o**) derivatives were the most active compounds for *S. aureus* ATCC 25923 (MIC = 1.95 –1.25 μg/mL) and *T. cruzi* (IC_{50} = 7.91 μM), respectively. Also, a preliminary evaluation against *C. albicans* involving some compounds was performed and the 5-(4-CH_3Ph, **5e**) derivative was the most active compound (MIC = 3.28–2.95 μg/mL). In this preliminary study, all synthesized 3-acetyl-2,5-disubstituted-2,3-dihydro-1,3,4-oxadiazole derivatives were active against all microorganisms tested.

1. Introduction

Although many efforts have been made, bacterial and protozoal infections are still responsible for high rates of morbidity and mortality throughout the world, being an important threat to the public health system, especially in the developing countries. It is estimated that about 15.7% of infections are caused by *Staphylococcus aureus*,[1] while *Trypanosoma cruzi* infections affect around 20,000 people per year,[2,3] and 21,000 deaths are attributed to Chagas' disease every year.[2]

The incidence of bacterial resistance to antibiotic therapy, including here the emergence of multidrug resistant pathogens, as well as the often poor safety profile and lack of efficacy of the currently available drugs, reinforces the need for the development of new and potent chemical entities or an improvement in the activity of well-known chemical compounds. Considering this statement, the synthesis of analogues can be seen as an efficient approach to optimize an active chemical structure and design new drugs, since simple structural changes can lead to better biological activities through modifications of physicochemical properties.

Since the 1940s, nitroheterocyclic compounds, including derivatives with a five-membered heterocyclic ring,[4] have been used as antibacterial[5] and antiprotozoal[6] agents and they constitute an important class of heterocyclic compounds presenting high biological activity levels. Other studies, in which the 2,3-dihydro-1,3,4-oxadiazoline ring was into the molecular structure, have indicated antimicrobial,[7] anticonvulsivant,[8] antifungal,[7] and anti-inflammatory[9] activity related to that structural moiety. The main advantage of the cyclization step, in synthesis, and the introduction of an acetyl group is the presence of an oxadiazole ring that may improve pharmacokinetic efficacy due to its increased ability to establish hydrogen bonding interactions and confer enhanced metabolic stability. Because of that, it could be considered as an important structural motif for designing new drugs.[10]

Previous studies[11,12] showed that molecular modification techniques applied to nitrocompounds is an advantageous strategy for the definition of potential new candidates regarding anti-infective chemotherapy. Thus, in this study, the purpose was the design, synthesis, and evaluation of the biological activity of a novel set of 3-acetyl-2,5-disubstituted-2,3-dihydro-1,3,4-oxadiazole derivatives as an alternative to overcome the currently anti-infective drugs' resistance and, consequently, to establish more effective therapies.

Additionally, a molecular modeling approach was carried out to identify possible qualitative property-activity relationships. For that, the lipophilic (LP) and electrostatic potential (EP) maps were

* Corresponding author. Tel.: +55 11 3091 3726; fax: +55 11 3815 6386.
E-mail address: marishii@usp.br (M. Ishii).

0968-0896/$ - see front matter © 2011 Elsevier Ltd. All rights reserved.
doi:10.1016/j.bmc.2011.09.009

the properties primarily considered. As it is well known, the lipophilicity or hydrophobicity property is quite important to the diffusion of any compound through the bacterial biological system. This property can generally be expressed by the calculated *n*-octanol/water partition coefficient (*C* log *P*). The map of EP is related to the electronic density distribution and considers, for example, the contribution of substituent groups to the whole molecular electronic density.

Moreover, the steric atomic hindrance was also calculated to verify the contribution of substituent volume and its relationship with the biological data.

2. Results and discussion

2.1. Chemistry

In this study, the synthesis of fifteen 3-acetyl-2,5-disubstituted-2,3-dihydro-1,3,4-oxadiazole derivatives was performed in four steps: the synthesis of 4-substituted methyl esters **(2a–o)** from commercially available substituted benzoic acids **(1a–o)**, synthesis of 4-substituted benzhydrazides **(3a–o)** from those methyl esters, synthesis of Schiff's bases **(4a–o)** from reaction with 5-nitro-2-thiophenecarboxaldehyde, and synthesis of 3-acetyl-2,5-disubstituted-2,3-dihydro-1,3,4-oxadiazole derivatives **(5a–o)** from the Schiff's bases (Fig. 1).

The synthesis of 4-substituted benzoic acid 4-substituted *N*′-((5-nitrothiophen-2-yl)methylene)benzohydrazide **(4a–o)** shown to be simple and practical, achieving yield in the range from 80% to 90%, as described in previous studies.[14] On the other hand, for the novel series of 3-acetyl-2,5-disubstituted-1,3,4-oxadiazoline derivatives (**5a**–**o**), the parameters of reaction time and temperature were adjusted for each compound. The minimal temperature for the product formation was 120 °C, considering that in less severe conditions the reaction time did not translate into a marked improvement for the reaction yield.

During the synthesis procedure, thin layer chromatography (TLC) analysis was performed to verify the formation of 3-acetyl-2,5-disubstituted-1,3,4-oxadiazolines. The structural elucidation of these derivatives was confirmed through ^{1}H NMR and ^{13}C NMR spectra analysis, considering chemical shifts (δ) related to the residual solvent signal or internal standard (tetramethylsilane). It was observed that the absence of a singlet signal around δ 12 ppm, indicating the proton of amidic nitrogen and a singlet at δ 7.74 ppm was the evidence of the 2,3-dihydro-1,3,4-oxadiazoline ring group formation. The presence of a singlet signal near to δ 2.29 ppm confirmed the three protons related to the acetyl group. Analyzing the ^{13}C NMR spectra, signals can be observed near to 168 and 21 ppm, which indicate the presence of carbonyl and alkyl group, respectively. The ^{1}H NMR, ^{13}C NMR, and elemental analysis data were in agreement with the proposed structures.

2.2. Biological activities and molecular modeling findings

The biological activities of 3-acetyl-2,5-disubstituted-2,3-dihydro-1,3,4-oxadiazole derivatives against *S. aureus* (ATCC 25923, SP3/R33, and VISA3 strains) were determined using the minimum inhibitory concentration (MIC) method. The percentage of growth inhibition for the *T. cruzi* epimastigote form (Y strain) was expressed as IC_{50} values, which represent the compound concentration responsible for inhibiting 50% of the parasite population growth. Results are shown in Table 1.

For the *S. aureus* ATCC strain, ampicillin was used as control drug. The MIC values indicated as the most and least active compounds the 4-OC_4H_9 (**5l**) and the 4-C_3H_7 (**5h**) substituted derivatives, respectively. The MIC values found for **5l** ranged from 1.95 to 1.25 μg/mL, and for **5h** varied from 4.61 to 3.28 μg/mL. The two compounds have a hydrophobic character as represented through the LP texture maps as well as expressed by the *C* log *P* values (see Fig. 2A and Table 2). The 4-OC_4H_9 and 4-C_3H_7 substituent groups do provide the same electronic features to the **5l** and **5h** compounds as can be visualized through the EP opaque maps (Fig. 2B). The 4-OC_4H_9 and 4-alkyl substituent have an electron donating effect on the aromatic ring (red to green color more delimited on the aromatic ring).

Indeed, as the alkyl chain length was increased the activity of 3-acetyl-2,5-disubstituted-1,3,4-oxadiazoline derivatives progressively decreased for the *S. aureus* ATCC strain [4-CH_3 (**5f**) ≫ 4-C_2H_5 (**5g**) ≫ 4-C_3H_7 (**5h**)] (Table 1). This trend might be explained by the molecular hydrophobicity and/or steric hindrance features. A longer alkyl chain could impair the approximation of enzymes, for example, which would be acting as potential targets. The

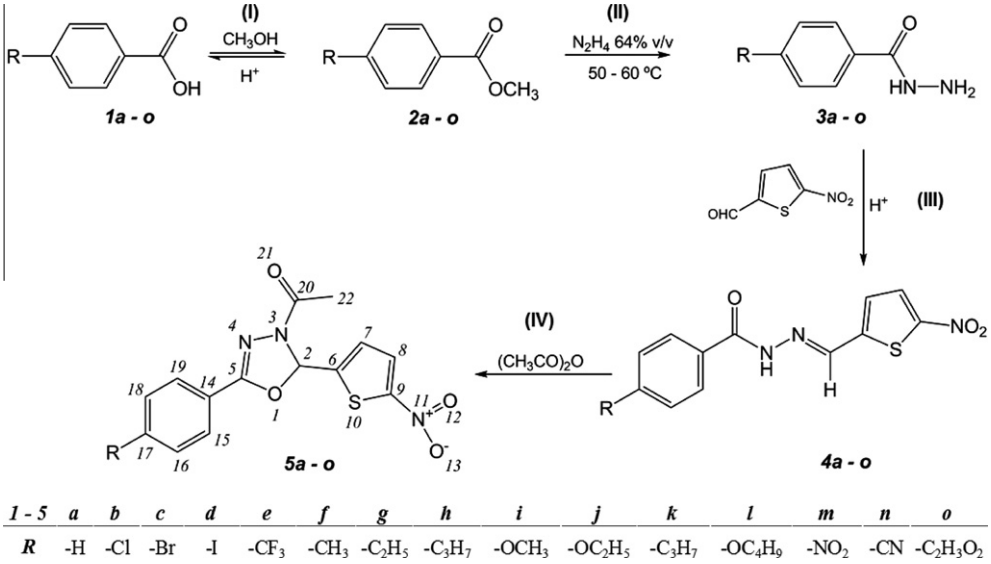

Figure 1. Synthesis of 3-acetyl-2,5-disubstituted-2,3-dihydro-1,3,4-oxadiazoles derivatives. Reaction conditions: (I): CH_3OH, H_2SO_4/reflux/4 h; (II): N_2H_4 64% aq/75 °C/10 min; (III) 5-nitro-2-thiophenecarboxaldehyde, H_2O, H_2SO_4, CH_3COOH, C_2H_5OH/reflux/1 h; (IV) acetic anhydride/120 °C/8 h.

Table 1
In vitro antibacterial and antiprotozoal activity of the series of 3-acetyl-2,5-disubstituted-2,3-dihydro-1,3,4-oxadiazole derivatives

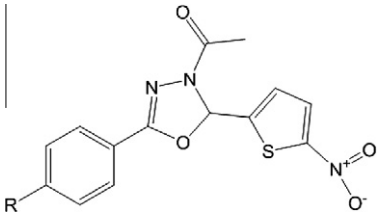

Compound	R	*Staphylococcus aureus*			*Trypanosoma cruzi*[c]
		ATCC 25923 MIC[d] (μg/mL)	SP3/R33[a] MIC[d] (μg/mL)	VISA3[a,b] MIC[d] (μg/mL)	IC_{50}[e] (μM)
5a	–H	3.07–2.46	2.50–1.25	1.25–0.63	10.24
5b	–Cl	2.46–1.97	2.50–1.25	5.00–2.50	10.85
5c	–Br	2.95–2.66	2.50–1.25	5.00–2.50	10.16
5d	–I	3.58–2.87	2.50–1.25	5.00–2.50	12.10
5e	$-CF_3$	3.28–2.62	2.50–1.25	5.00–2.50	14.25
5f	$-CH_3$	3.28–2.62	2.50–1.25	5.00–2.50	11.47
5g	$-C_2H_5$	3.36–2.69	2.50–1.25	5.00–2.50	10.74
5h	$-C_3H_7$	4.61–3.28	2.50–1.25	2.50–1.25	9.90
5i	$-OCH_3$	2.79–2.23	2.50–1.25	1.25–0.63	10.67
5j	$-OC_2H_5$	2.95–2.36	2.50–1.25	5.00–2.50	26.64
5k	$-OC_3H_7$	4.10–3.28	5.00–2.50	5.00–2.50	12.20
5l	$-OC_4H_9$	1.95–1.25	2.50–1.25	10.00–5.00	11.47
5m	$-NO_2$	2.66–2.39	5.00–2.50	2.50–1.25	9.85
5n	–CN	2.95–2.66	2.50–1.25	1.25–0.63	8.19
5o	$-CO_2CH_3$	3.38–2.95	2.50–1.25	1.25–0.63	7.91
Nifuroxazide		6.59–5.90	–	10.00–5.00	120.46
Ampicilin		0.10–0.20	32.00–16.00	32.00–16.00	–
Vancomycin		–	1.00–0.50	1.00–0.50	–
Benznidazole		–	–	–	20.84

[a] Resistant to amoxicilin/clavulanic acid, ampicilin, cephazoline, cephotaxime, cephalotine, ciprofloxacin, clindamycin, erythromycin, gentamicin, imipenem, nitrofurantoin, norfloxacin, oxacillin, penicillin, rifampicin, trimethoprim/sulfametoxazole.
[b] Vancomycin-intermediate *Staphylococcus aureus* strain.
[c] Epimastigote form of Y strain.
[d] Values corresponding to the average of three repetitions.
[e] Concentration of compound which causes 50% parasite growth inhibition.

calculated steric hindrance[15] values found for the alkyl substituent 4-CH_3, 4-C_2H_5, and 4-C_3H_7 were 3.46, 6.26, and 9.15, respectively. The van der Waals volumes of these substituent groups can be visualized in Figure 3.

Regarding the alkoxy derivatives, the same behavior was observed for the *S. aureus* ATCC strain when the alkyl chain length was increased up to three carbon atoms [4-OCH_3 (**5i**) ≫ 4-OC_2H_5 (**5j**) ≫ 4-OC_3H_7 (**5k**)] (see Table 1). The calculated steric hindrance values found for the alkoxy substituent 4-OCH_3, 4-OC_2H_5, and 4-OC_3H_7 were 4.47, 7.20, and 10.07, respectively, corroborating for that assumption (see Fig. 3). For biological activity evaluation, as the bioactivity was, measured using MIC method, none specific target was actually addressed.

Otherwise, the calculated partition coefficient (*C* log *P*), is the major factor in the permeability of the tested compound through the cell membrane and can be directly related to the produced biological effect.[20] According to Table 2, the *C* log *P* values found for the compounds **5f**, **5g**, and **5h** were 1.47, 1.93, and 2.38, respectively. The compounds **5i**, **5j**, and **5k** presented *C* log *P* values of 0.97, 1.32, and 1.84, correspondingly. As expected, the presence of a polar heteroatom at the 4-alkyl substituent group decreased the global hydrophobicity of the 3-acetyl-2,5-disubstituted-1,3,4-oxadiazoline derivatives. Visually, regarding the LP texture maps (see Fig. 4), which are intimately related to the *C* log *P* values, the dark brown color on the region of the 4-alkyl substituent group was in general replaced by a green to light brown color in comparison to the 4-alkoxy moiety.

The compounds 4-Cl (**5b**), 4-OCH_3 (**5i**), 4-OC_2H_5 (**5j**), 4-OC_4H_9 (**5l**), 4-NO_2 (**5m**), and 4-CN (**5n**) presented higher bioactivity than the non-substituted compound (**5a**), indicating that molecular structural modifications, specially as in the synthesis of analogs, correspond to an advantageous strategy for obtaining more effective therapeutic alternatives. A quantitative structure–activity relationship study is currently in progress to provide more information and understanding of the mechanism of action of these derivatives.

Ampicillin and vancomycin were used as control drugs for the *S. aureus* SP3/R33 and VISA3 strains, respectively. The MIC values were the same for all synthesized compounds when they were tested against the *S. aureus* SP3/R33 strain (2.50–1.25 μg/mL), except for the 4-OC_3H_7 (**5k**) and 4-NO_2 (**5m**) derivatives (Table 1). The compound **5m** presented the lowest *C* log *P* value (−1.32, see Table 2), which is probably due to the hydrophilic character attributed to its substituent group (4-NO_2) by the calculation method. None conclusive explanation regarding the MIC values found for the *S. aureus* SP3/R33 strain can be made based upon the substituent groups or related physicochemical properties pointed out here.

Again, for the *S. aureus* VISA3 strain, the MIC values did not change significantly, and ranged mostly from 5.00 to 2.50 μg/mL, except for the 4-OC_4H_9 (**5l**) derivative (10.00–5.00 μg/mL) (Table 1). This finding might suggest that when the alkoxy substituent group presents more than three carbon atoms in its chain the activity against the VISA3 strain could be reduced. The 4-OC_4H_9 substituent group has a steric atomic hindrance value of 12.99, which is bigger than those found for the 4-OC_2H_5 and 4-OC_3H_7 derivatives (7.20 and 10.07, respectively). The compounds 4-OCH_3 (**5i**), 4-CN (**5n**), 4-CO_2CH_3 (**5o**), and the non-substituted compound (5**a**) showed

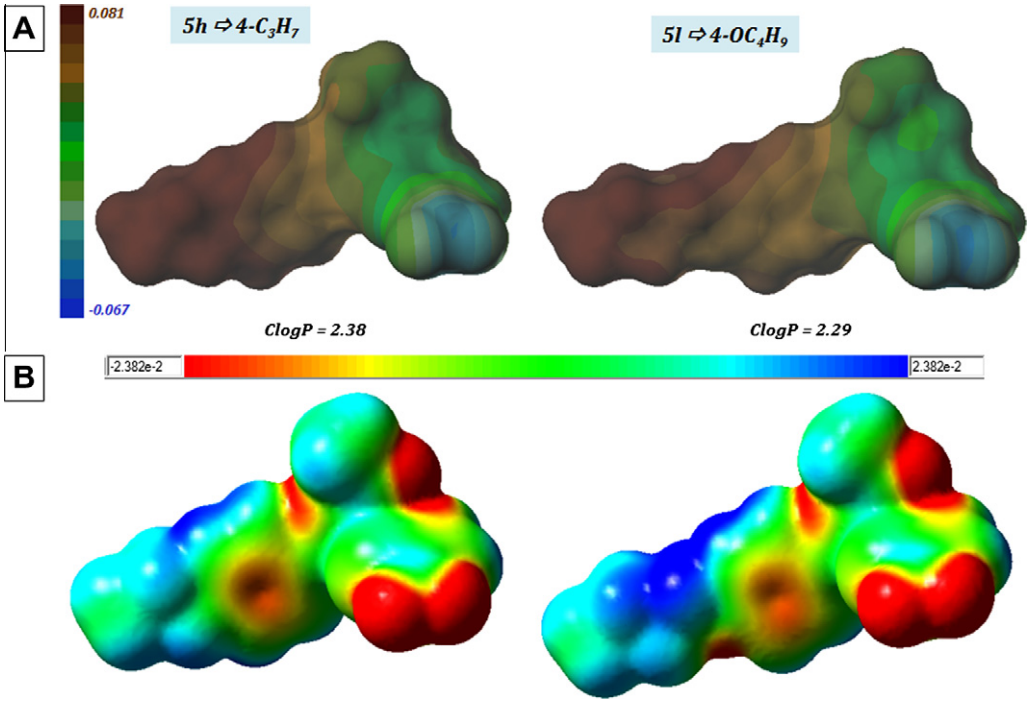

Figure 2. Comparison of the physicochemical properties calculated for the 4-C_3H_7 (**5h**) and 4-OC_4H_9 (**5l**) substituted derivatives. (A) LP texture maps and *C* log *P* values (Sybyl 8.0 package).[18] Brown color (0.081) indicates hydrophobic regions and blue color (−0.067) denotes hydrophilic areas. (B) EP opaque maps using GaussView 3.0 (Gaussian Inc. 1993–2003). Red color indicates negative values of EP (−0.024) or higher electronic density regions while blue color denotes positive values (0.024) or lower electronic density distribution areas.

Table 2
C log *P* values found for the series of 3-acetyl-2,5-disubstituted-2,3-dihydro-1,3,4-oxadiazole derivatives using Ghose et al. method (1998)[16] and SLN[17] (Sybyl 8.0[18])

Compound	–R	*C* log *P* values
5a	–H	0.98
5b	–Cl	1.65
5c	–Br	1.73
5d	–I	1.56
5e	$-CF_3$	1.93
5f	$-CH_3$	1.47
5g	$-C_2H_5$	1.93
5h	$-C_3H_7$	2.38
5i	$-OCH_3$	0.97
5j	$-OC_2H_5$	1.32
5k	$-OC_3H_7$	1.84
5l	$-OC_4H_9$	2.29
5m	$-NO_2$	−1.32
5n	–CN	0.82
5o	$-CHCO_2$	0.71

the same activity and the lowest MIC values (see Table 1). Additionally, they presented *C* log *P* values between zero and one [0.97 (**5i**), 0.82 (**5n**), 0.71(**5o**), and 0.98 (**5a**)] (Table 2), which could indicate a preferential range for the hydrophobicity feature regarding the bioactivity against the VISA3 strain.

Observing the biological data, it could be hypothesized that the molecular recognition process between the set of 3-acetyl-2,5-disubstituted-2,3-dihydro-1,3,4-oxadiazole derivatives (ligands) and the multidrug-resistant strains, SP3/R33 and VISA3 (targets), would be distinct since different ranges of MIC values were found.

The most active compound against the epimastigote form of *T. cruzi* was the 4-CO_2CH_3 (**5o**) derivative (IC_{50} value of 7.91 μM). The **5o** compound was threefold more active than **5j** (4-OC_2H_5), the less active compound (IC_{50} value of 26.64 μM) (Table 1). The 4-CO_2CH_3 (**5o**) and 4-OC_2H_5 (**5j**) derivatives present steric hindrance values of 5.86 and 7.20, respectively. Also, the **5o** compound has a more hydrophilic character in comparison to **5j** (see Table 2, *C* log *P* values). Considering the data found for the *T. cruzi* epimastigote form, when the length of alkoxy chain was increased the biological activity did not progressively decrease. The 4-OC_3H_7 (**5k**) and 4-OC_4H_9 (**5l**) derivatives presented IC_{50} values of 12.20 and 11.47 μM, respectively.

Some of the tested compounds showed antiprotozoal biological activity equivalent to the non-substituted compound (**5a**), following the trend observed for the multidrug-resistant *S. aureus* strains. The 4-OCH_3 (**5i**) derivative, for example, presented a *C* log *P* value quite similar to the non-substituted compound (**5a**), which probably reflected in its anti-*T. cruzi* activity. The LP texture maps of the compounds **5a** and **5i** are showed in Figure 5. All compounds were more active than benznidazole at the same assay conditions.

An initial screening for the antifungal activity of these compounds established MIC ranges of values from 8.00 to 7.20 μg/mL for the 4-CF_3 (**5e**) derivative; from 7.20 to 6.78 μg/mL for 4-OC_4H_9 (**5l**); from 6.48 to 5.83 μg/mL for 4-OC_2H_5 (**5j**); from 4.72 to 4.25 μg/mL for 4-Cl (**5b**); and from 3.28 to 2.95 μg/mL for 4-CH_3 (**5f**), which was the most active antifungal agent tested. The concentration ranges used for the determination of antifungal activity varied depending upon the solubility of the compound in the medium used.

Considering the calculated properties, the most (**5f**) and the least (**5e**) active compounds have a hydrophobic character, expressed by the *C* log *P* values and visually represented by the LP texture maps (see Fig. 6B). The steric atomic hindrance contributions found for the 4-CF_3 (**5e**) and 4-CH_3 (**5f**) substituent groups were 2.82 and 3.41, respectively, indicating that there is not a significant difference for this geometrical or structural feature (Fig. 6C). Otherwise, the electronic property is indeed distinct regarding the two substituent groups. The 4-CH_3 (**5f**) substituent group has an inductive electron donating effect on the aromatic system (red to yellow color on the aromatic ring—Fig.6A) whereas the 4-CF_3 (**5e**) substituent group presents an inductive electron

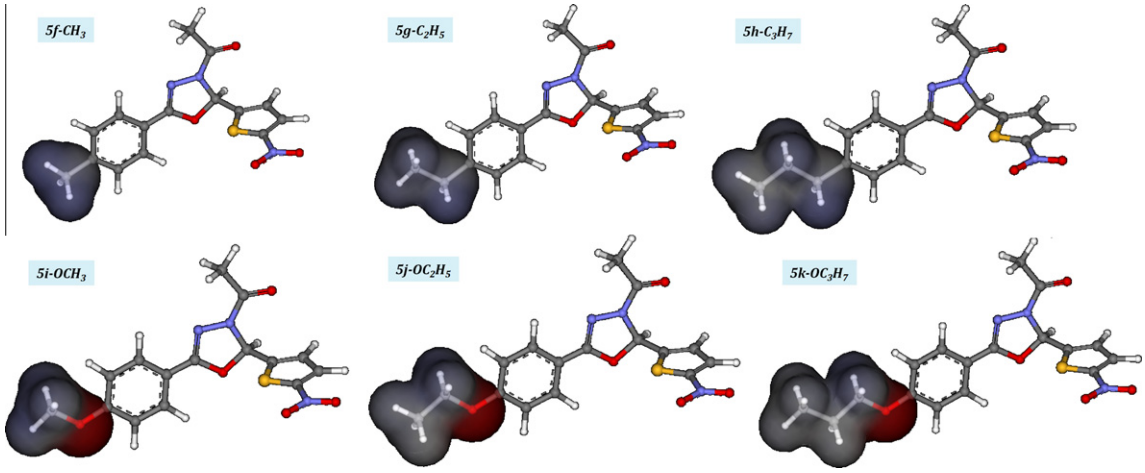

Figure 3. Visualization of the substituent groups' volumes through van der Waals surfaces (ViewerLite 5.0, Accelrys Inc. 2002) for the compounds **5f–k**. The molecules are displayed in ball-stick scaled model (carbon atoms are in gray color, oxygen in red, nitrogen on blue, sulfur in yellow, and hydrogen atoms in white).

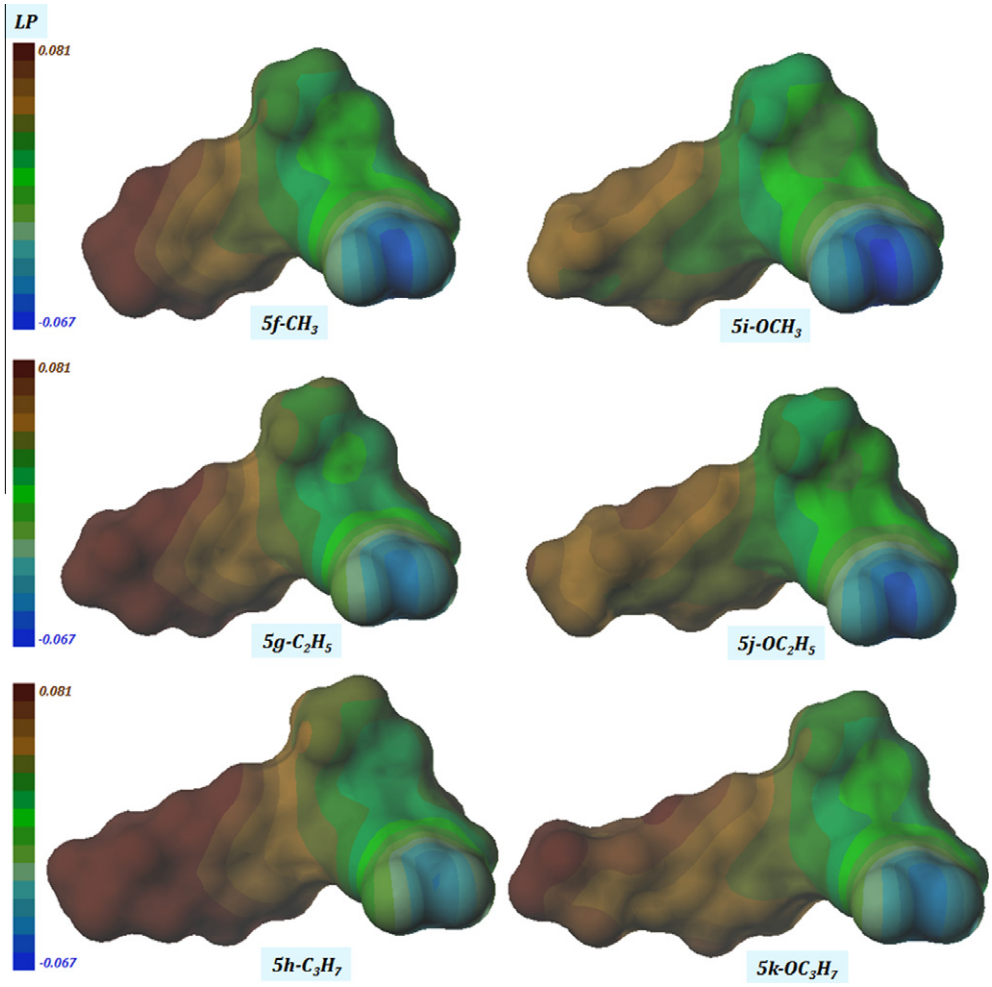

Figure 4. LP texture maps calculated for the compounds **5f–k** using the Sybyl 8.0 package.[18] Brown color (0.081) indicates hydrophobic regions and blue color (−0.067) denotes hydrophilic areas.

withdrawing effect on that molecule moiety (green color on the aromatic ring—Fig. 6A).

Although the MIC and IC_{50} values of the new oxadiazoline compounds presented in this study showed lower activity than the antibiotic drugs used as reference, they present a remarkable and wide spectrum of activity, which will be more efficiently explored through the addition of more compounds to this series.

Thus, in order to elucidate the bioactivity profile of this new class of compounds, the extension of the series of analogues is ongoing, and it is expected to provide a better understanding of

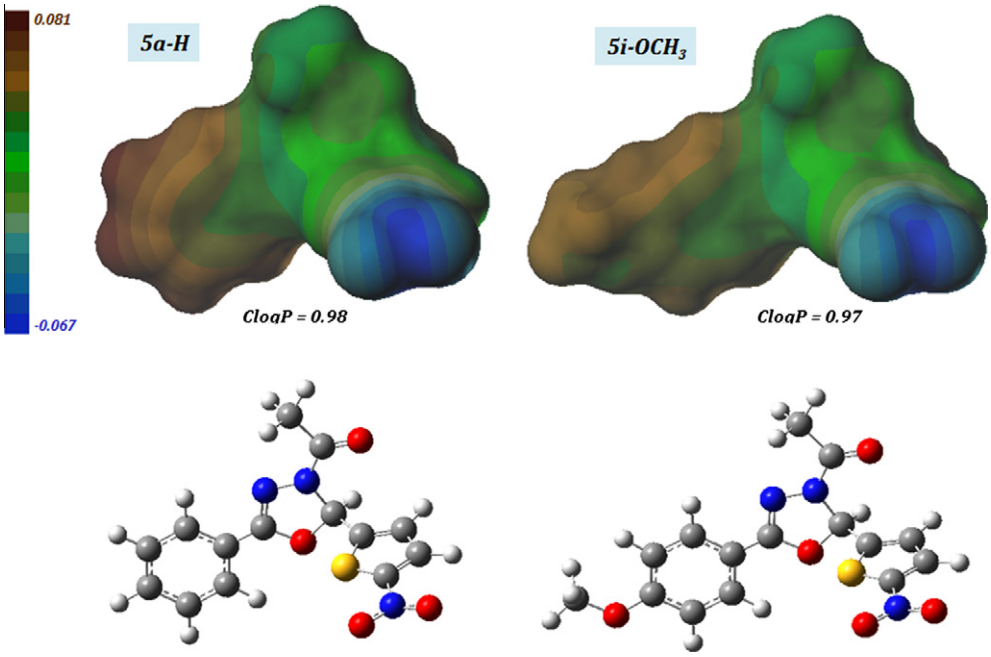

Figure 5. LP texture maps and *C* log *P* values found for the compound **5a** and **5i** using the Sybyl 8.0 package.[18] Brown color (0.081) indicates hydrophobic regions and blue color (−0.067) denotes hydrophilic areas. The molecules are displayed in ball-stick model (carbon atoms are in gray color, oxygen in red, nitrogen on blue, sulfur in yellow, and hydrogen atoms in white) (GaussView 3.0, Gaussian Inc. 1993–2003).[38]

the relationships between the 4-substitutent groups, their physicochemical properties, and the overall microbial activity.

3. Conclusion

Biological screening results showed that some compounds have a promising profile to be considered as attractive chemical entities for the development of new antiprotozoal and antibacterial agents. The 4-OC_4H_9 (**5l**) derivative was the most active compound against the *S. aureus* ATCC 25923 strain, while the 4-OCH_3 (**5i**), 4-CN (**5n**), and 4-CO_2CH_3 (**5o**) derivatives exhibited good activity against the VISA3 (SP3/R33) strain, similarly to the non-substituted compound and close to vancomycin. Regarding the initial assays for the *C. albicans* strain, the 4-CH_3 (**5f**) and the 4-Cl (**5b**) derivatives were showed as more active compounds. Their MIC ranges varied from 3.28 to 2.95 μg/mL and from 4.72 to 4.25 μg/mL, respectively, two-fold more active than 4-CF_3 (**5e**), 4-OC_4H_9 (**5l**), and 4-OC_2H_5 (**5j**). Further studies are needed to confirm these in vitro results and investigate the mode of action of these derivatives. The calculated physicochemical and structural properties, using molecular modeling techniques, provided suitable information to explain the resulting biological data allowing the establishment of qualitative property-activity relationships.

4. Experimental

4.1. Chemistry

NMR spectra were recorded on a BRUKER ADPX Advanced (300 MHz) spectrometer employing DMSO-d_6 solutions with tetramethylsilane as internal standard. Melting points were determined using Micro-Química MQAPF-301 apparatus and elemental analysis was performed on a Perkin-Elmer 24013 CHN Elemental Analyzer.

4.1.1. General procedure for the synthesis of methyl esters (2a–o)[20]

Each substituted benzoic acid **(1)** (0.04 mol) was heated at reflux for 4 hours in 50.0 mL (1.23 mol) of anhydrous methanol and 1.0 mL (2.0 mmol) of sulfuric acid. The solvent was concentrated and the product obtained washed with cold water. In some cases, as for non-substituted compounds, the ester showed an oily aspect and, to promote its precipitation, the compound was cooled by immersion in dry ice–ethanol bath.

4.1.2. General procedure for the synthesis of benzhydrazides (3a–o)[20]

Hydrazine hydrate 64% (v/v) (30.0 mL, 0.33 mol) was heated up to 50–60 °C. The methyl ester **3** (0.01 mol) was added and the mixture was heated at reflux for 10 min. The cooling was performed sequentially in water bath, followed by ice bath and dry ice–ethanol bath. The precipitate was filtered and washed with cold water.

4.1.3. General procedure for the synthesis of Schiff's bases (4a–o)

Schiff's bases were synthesized by heating at reflux 5-nitrothiophen-2-carboxaldehyde (0.01 mol) and benzhydrazides (**3**) (0.01 mol) in water, sulfuric acid, acetic acid, and methanol (8:7:8:20 v/v) for 1 h. After cooling, the mixture was poured into cold water to precipitate the Schiff's bases.

4.1.4. General procedure for the synthesis of 2,3-dihydro-1,3,4-oxadiazolines derivatives (5a–o)

0.5 g of the corresponding Schiff's base was dissolved in 100 mL acetic anhydride at 85 °C and the mixture heated at 120 °C for 8 h. The reaction medium was evaporated to 10% volume then cooled, allowing the product to precipitate.

4.1.4.1. 3-Acetyl-5-phenyl-2-(5-nitrothiophen-2-yl)-2,3-dihydro-1,3,4-oxadiazole (5a). White solid (72%); mp 103.0–104.0 °C. ^{1}H NMR (DMSO-d_6, 300 MHz): δ (ppm): 8.07 (d, 1H, H8, J = 4.3 Hz), 7.87 (d, 2H, H15,19, J = 8.6 Hz), 7.63 (s, 1H, H2), 7.56 (m, 3H, H16/17/18), 7.47 (d, 1H, H7, J = 4.3 Hz), 2.29 (s, 3H, H22); ^{13}C NMR {H} (DMSO-d_6, 75 MHz): δ (ppm): 167.3 (C20), 154.4 (C5), 151.6 (C6), 146.6 (C9), 132.2 (C14), 129.5 (C17), 129.1 (C16, C18), 127.1 (C8), 126.6 (C15, C19), 123.2 (C7), 86.7 (C2), 20.9 (C22); Anal. Calcd for ($C_{14}H_{11}N_3O_4S$): C, 52.99; H, 3.49; N, 13.24. Found: C, 53.06; H, 3.59; N, 13.24.

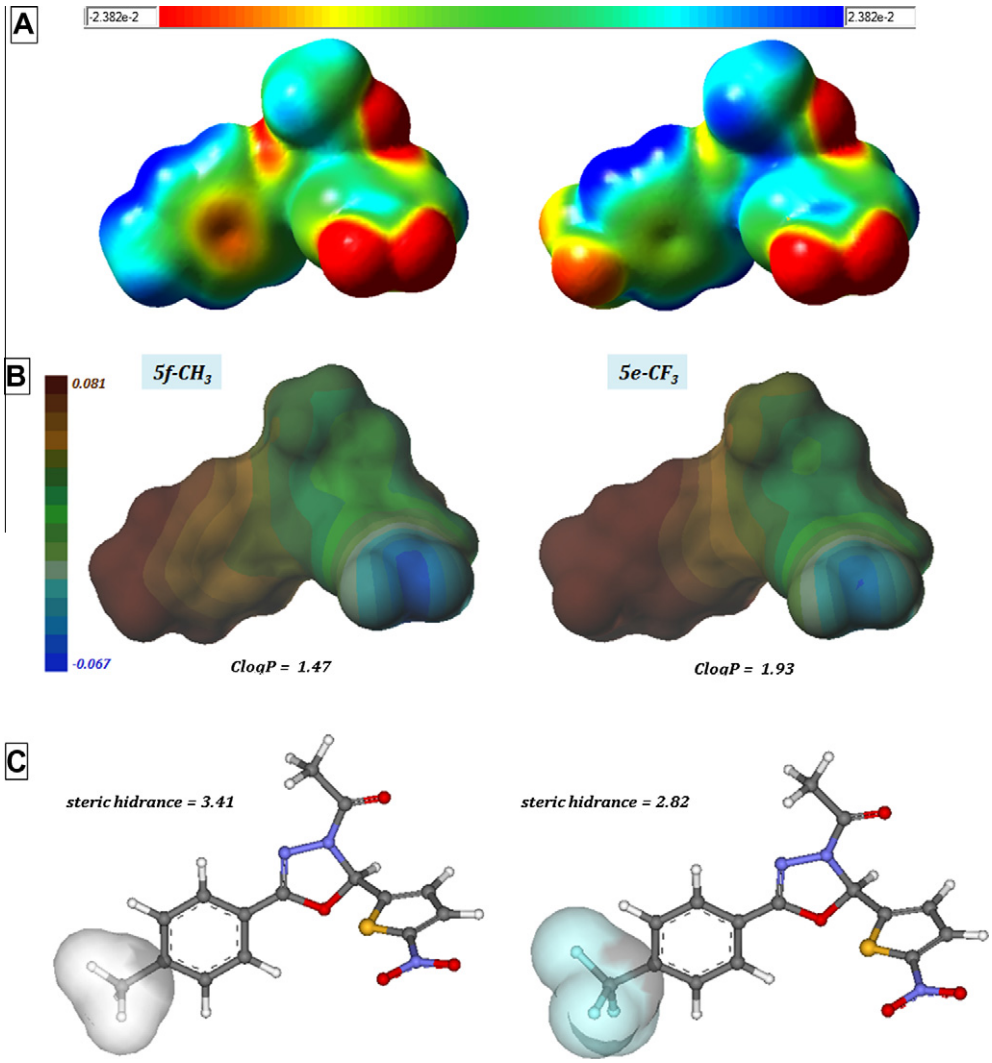

Figure 6. Comparison of the physicochemical and structural properties calculated for the 4-CH_3 (**5f**) and 4-CF_3 (**5e**) substituted derivatives. (A) EP opaque maps using GaussView 3.0 (Gaussian Inc. 1993–2003).[38] Red color indicates higher electronic density regions (−0.024) while blue color denotes lower electronic density areas (0.024). (B) LP texture maps and *C* log *P* values (Sybyl 8.0 package).[18] Brown color (0.081) indicates hydrophobic regions and blue color (−0.067) denotes hydrophilic areas. (C) Visualization of the substituent groups' volumes through van der Waals surfaces (ViewerLite 5.0, Accelrys Inc. 2002) and respective steric atomic hindrance values.[19] The molecules are displayed in ball-stick scaled model (carbon atoms are in gray color, oxygen in red, nitrogen on blue, sulfur in yellow, fluorine in cyan, and hydrogen atoms in white).

4.1.4.2. 3-Acetyl-5-(4-chlorophenyl)-2-(5-nitrothiophen-2-yl)-2,3-dihydro-1,3,4-oxadiazole (5b). Yellow solid (70%); mp 130.0–131.0 °C. ^{1}H NMR (DMSO-d_6, 300 MHz): δ (ppm): 8.08 (d, 1H, H8, J = 4.3 Hz), 7.87 (d, 2H, H15/19, J = 8.1 Hz), 7.63 (d, 2H, H16/18, J = 8.2 Hz), 7.58 (s, 1H, H2), 7.48 (d, 1H, H7, J = 4.3 Hz), 2.29 (s, 3H, H22); ^{13}C NMR {H} (DMSO-d_6, 75 MHz): δ (ppm): 167.4 (C20), 153.6 (C5), 151.6 (C6), 146.4 (C9), 136.9 (C17), 129.5 (C14), 129.3 (C15, C19), 128.4 (C16, C18), 127.1 (C8), 122.1 (C7), 87.0 (C2), 20.9 (C22); Anal. Calcd for ($C_{14}H_{10}ClN_3O_4S$): C, 47.80; H, 2.87; N, 11.95. Found: C, 47.88; H, 2.67; N, 11.95.

4.1.4.3. 3-Acetyl-5-(4-bromophenyl)-2-(5-nitrothiophen-2-yl)-2,3-dihydro-1,3,4-oxadiazole (5c). Yellow solid (42%); mp 142.0–143.0 °C. ^{1}H NMR (DMSO-d_6, 300 MHz): δ (ppm): 8.01 (d, 1H, H8, J = 4.3 Hz), 7.74 (d, 2H, H15/19, J = 9.0 Hz), 7.70 (d, 2H, H16/18, J = 9.0 Hz), 7.51 (s, 1H, H2), 7.42 (d, 1H, H7, J = 4.3 Hz), 2.23 (s, 3H, H22); ^{13}C NMR {H} (DMSO-d_6, 75 MHz): δ (ppm): 167.9 (C20), 154.3 (C5), 152.2 (C6), 147.0 (C9), 132.7 (C16, C18), 129.9 (C14), 129.0 (C15, C19), 127.6 (C8), 126.3 (C7), 123.0 (C17), 87.6 (C2), 21.5 (C22); Anal. Calcd for ($C_{14}H_{10}BrN_3O_3S$): C, 42.44; H, 2.54; N, 10.61. Found: C, 42.38; H, 2.57; N, 10.63.

4.1.4.4. 3-Acetyl-5-(4-iodophenyl)-2-(5-nitrothiophen-2-yl)-2,3-dihydro-1,3,4-oxadiazole (5d). Yellow solid (55%); mp 156.0–157.0 °C. ^{1}H NMR (DMSO-d_6, 300 MHz): δ (ppm): 8.07 (d, 1H, H8, J = 4.1 Hz), 7.94 (d, 2H, H16/18, J = 8.6 Hz), 7.62 (d, 2H, H15/19, J = 8.6 Hz), 7.57 (s, 1H, H2), 7.47 (d, 1H, H7, J = 4.3 Hz), 2.29 (s, 3H, H22); ^{13}C NMR {H} (DMSO-d_6, 75 MHz): δ (ppm): 167.4 (C20), 154.0 (C5), 151.7 (C6), 146.5 (C9), 138.0 (C16, C18), 129.5 (C14), 128.3 (C15, C19), 127.2 (C8), 127.2 (C8), 122.7 (C7), 99.9 (C2), 21.0 (C22); Anal. Calcd for ($C_{14}H_{10}IN_3O_4S$): C, 37.94; H, 2.27; N, 9.48. Found: C, 37.89; H, 2.29; N, 9.37.

4.1.4.5. 3-Acetyl-5-(4-trifluoromethylphenyl)-2-(5-nitrothiophen-2-yl)-2,3-dihydro-1,3,4-oxadiazole (5e). Yellow solid (59%); mp 135.0–136.0 °C. ^{1}H NMR (DMSO-d_6, 300 MHz): δ (ppm): 8.08 (d, 1H, H8, J = 4.3 Hz), 8.07 (d, 2H, H15/19, J = 8.4 Hz), 7.93 (d, 2H, H16/18, J = 8.4 Hz), 7.62 (s, 1H, H2), 7.51 (d, 1H, H7, J = 4.3 Hz), 2.31 (s, 3H, H22); ^{13}C NMR {H} (DMSO-d_6, 75 MHz): δ (ppm): 168.1 (C20), 153.8 (C5), 152.2 (C6), 146.8 (C9), 132.4 (C14), 131.9 (C17), 130.0 (C15, C19), 128.0 (C16, C18), 127.8 (C8), 126.7 (C7), 126.6 (CF_3), 87.9 (C2), 21.5 (C22); Anal. Calcd for ($C_{15}H_{10}F_3N_3O_4S$): C, 46.76; H, 2.62; N, 10.91. Found: C, 46.90; H, 2.92; N, 11.02.

4.1.4.6. 3-Acetyl-5-(4-methylphenyl)-2-(5-nitrothiophen-2-yl)-2,3-dihydro-1,3,4-oxadiazole (5f). Yellow solid (48%); mp 127.0–128.0 °C. ^{1}H NMR (DMSO-d_6, 300 MHz): δ (ppm): 8.07 (d, 1H, H8, J = 4.3 Hz), 7.76 (d, 2H, H15/19, J = 7.9 Hz), 7.55 (s, 1H, H2), 7.46 (d, 1H, H7, J = 4.3 Hz), 7.37 (d, 2H, H16/18, J = 7.9 Hz), 2.39 (s, 3H, CH_3), 2.29 (s, 3H, H22); ^{13}C NMR {H} (DMSO-d_6, 75 MHz): δ (ppm): 167.2 (C20), 154.6 (C5), 151.6 (C6), 146.7 (C9), 142.5 (C17), 129.7 (C16, C18), 129.5 (C14), 127.0 (C8), 126.6 (C15, C19), 120.4 (C7), 86.6 (C2), 21.1 (C22), 21,0 (CH3); Anal. Calcd for ($C_{15}H_{13}N_3O_4S$): C, 54.37; H, 3.95; N, 12.68. Found: C, 54.21; H, 4.03; N, 12.58.

4.1.4.7. 3-Acetyl-5-(4-ethylphenyl)-2-(5-nitrothiophen-2-yl)-2,3-dihydro-1,3,4-oxadiazole (5g). Yellow solid (62%); mp 108.0–109.0 °C. ^{1}H NMR (DMSO-d_6, 300 MHz): δ (ppm): 8.06 (d, 1H, H8, J = 4.1 Hz), 7.79 (d, 2H, H16/18, J = 8.1 Hz), 7.56 (s, 1H, H2), 7.46 (d, 1H, H7, J = 4.3 Hz), 7.39 (d, 2H, H15,19, J = 8.1 Hz), 2.68 (m, 2H, CH_2, 7.1 Hz), 2.29 (s, 3H, H22), 1.17 (t, 3H, CH_3, J = 7.1 Hz); ^{13}C NMR {H} (DMSO-d_6, 75 MHz): δ (ppm): 167.7 (C20), 155.1 (C5), 152.1 (C6), 149.0 (C9), 147.3 (C17), 130.02 (C14), 129.0 (C15, C19), 127.5 (C8), 127.3 (C16, C18), 121.2 (C7), 87.1 (C2), 28.6 (CH_2), 21.49 (C22), 15.5 (CH_3); Anal. Calcd for ($C_{16}H_{15}N_3O_4S$): C, 55.64; H, 4.38; N, 12.17. Found: C, 55.58; H, 4.54; N, 11.98.

4.1.4.8. 3-Acetyl-5-(4-*n*-propylphenyl)-2-(5-nitrothiophen-2-yl)-2,3-dihydro-1,3,4-oxadiazole (5h). White solid (65%); mp 73.0–74.0 °C. ^{1}H NMR (DMSO-d_6, 300 MHz): δ (ppm): 8.06 (d, 1H, H8, J = 4.0 Hz), 7.78 (d, 2H, H15/19, J = 8.1 Hz), 7.56 (s, 1H, H2), 7.46 (d, 1H, H7, J = 4.0 Hz), 7.37 (d, 2H, H18,16, J = 8.1 Hz), 2.62 (t, 2H, CH_2, J = 7.6 Hz), 2.28 (s, 3H, H22), 1.62 (m, 2H, CH_2, J = 7.3 Hz), 0.89 (t, 3H, CH_3, J = 7.2 Hz); ^{13}C NMR {H} (DMSO-d_6, 75 MHz): δ (ppm): 167.2 (C20), 154.6 (C5), 151.6 (C6), 146.9 (C9), 146.7 (C17), 129.5 (C14), 129.1 (C15, C19), 127.0 (C8), 126.6 (C16, C18), 120.71 (C7), 86.6 (C2), 37.1 (CH_2), 23.67 (CH_2), 21.0 (C22), 13.5 (CH_3); Anal. Calcd for ($C_{17}H_{17}N_3O_4S$): C, 56.81; H, 4.77; N, 11.69. Found: C, 57.13; H, 5.11; N, 11.72.

4.1.4.9. 3-Acetyl-5-(4-methoxyphenyl)-2-(5-nitrothiophen-2-yl)-2,3-dihydro-1,3,4-oxadiazole (5i). White solid (51%); mp 109.0–110.0 °C. ^{1}H NMR (DMSO-d_6, 300 MHz): δ (ppm): 8.08 (d, 1H, H8, J = 4.3 Hz), 7.82 (d, 2H, H15/19, J = 8.8 Hz), 7.56 (s, 1H, H2), 7.47 (d, 1H, H7, J = 4.1 Hz), 7.12 (d, 2H, H16/18, J = 8.6 Hz), 3.9 (s, 3H, OCH_3), 2.29 (s, 3H, H22); ^{13}C NMR {H} (DMSO-d_6, 75 MHz): δ (ppm): 167.2 (C20), 162.3 (C17), 154.5 (C5), 151.6 (C6), 146.9 (C9), 129.5 (C8), 128.6 (C15, C19), 127.0 (C7), 115.4 (C14), 114.6 (C16, C18), 86.5 (C2), 55.5 (OCH_3), 21.0 (C22); Anal. Calcd for ($C_{15}H_{13}N_3O_5S$): C, 51.87; H, 3.77; N, 12.10. Found: C, 51.75; H, 3.69; N, 11.87.

4.1.4.10. 3-Acetyl-5-(4-ethoxyphenyl)-2-(5-nitrothiophen-2-yl)-2,3-dihydro-1,3,4-oxadiazole (5j). Yellow solid (56%); mp 108.0–109.0 °C. ^{1}H NMR (DMSO-d_6, 300 MHz): δ (ppm): 8.07 (d, 1H, H8, J = 4.3 Hz), 7.79 (d, 2H, H15/19, J = 8.6 Hz), 7.54 (s, 1H, H2), 7.45 (d, 1H, H7, J = 4.3 Hz), 7.08 (d, 2H, H16/18, J = 8.6 Hz), 4.11 (q, 2H, CH_2, J = 6.9 Hz), 2.27 (s, 3H, H22), 1.35 (t, 3H, CH_3, J = 6.9 Hz); ^{13}C NMR {H} (DMSO-d_6, 75 MHz): δ (ppm): 167.6 (C20), 162.0 (C17), 155.0 (C5), 152.0 (C6), 147.4 (C9), 130.0 (C8), 129.1 (C15, C19), 127.7 (C7), 127.5 (C14), 115.5 (C16, C18), 86.9 (C2), 64.0 (CH_2), 21.5 (C22), 14.9 (CH_3); Anal. Calcd for ($C_{16}H_{15}N_3O_5S$): C, 53.18; H, 4.18; N, 11.63. Found: C, 52.73; H, 3.91; N, 11.20.

4.1.4.11. 3-Acetyl-5-(4-*n*-propoxyphenyl)-2-(5-nitrothiophen-2-yl)-2,3-dihydro-1,3,4-oxadiazole (5k). White solid (50%); mp 102.0–103.0 °C. ^{1}H NMR (DMSO-d_6, 300 MHz): δ (ppm): 8.07 (d, 1H, H8, J = 4.3 Hz), 7.79 (d, 2H, H15/19, J = 9.0 Hz), 7.54 (s, 1H, H2), 7.45 (d, 1H, H7, J = 4.3 Hz), 7.10 (d, 2H, H16/18, J = 9.0 Hz), 4.01 (t, 2H, CH_2, J = 6.3 Hz), 2.27 (s, 3H, H22), 1.75 (m, 2H, CH_2, J = 7.2 Hz), 0.98 (t, 3H, CH_3, J = 7.2 Hz); ^{13}C NMR {H} (DMSO-d_6, 75 MHz): δ ppm): 167.6 (C20), 162.2 (C17), 155.1 (C5), 152.0 (C6), 147.3 (C9), 130.0 (C8), 115.5 (C7), 129.1 (C15, C19), 127.5 (C14), 129.0 (C16, C18), 86.9 (C2), 69.8 (CH_2), 22.3 (CH_2), 21.5 (C22), 10.7 (CH_3); Anal. Calcd for ($C_{17}H_{17}N_3O_5S$): C, 54.39; H, 4.56; N, 11.19. Found: C, 54.50; H, 4.56; N, 11.14.

4.1.4.12. 3-Acetyl-5-(4-*n*-butoxyphenyl)-2-(5-nitrothiophen-2-yl)-2,3-dihydro-1,3,4-oxadiazole (5l). Yellow solid (32%); mp 116.0–117.0 °C. ^{1}H NMR (DMSO-d_6, 300 MHz): δ (ppm): 8.07 (d, 1H, H8, J = 4.3 Hz), 7.78 (d, 2H, H15/19, J = 9.0 Hz), 7.53 (s, 1H, H2), 7.45 (d, 1H, H7, J = 4.2 Hz), 7.08 (d, 2H, H16/18, J = 9.0 Hz), 4.05 (t, 2H, CH_2, J = 6.4 Hz), 2.27 (s, 3H, H22), 1.72 (m, 2H, CH_2, J = 6.6 Hz), 1.40 (m, CH_2, J = 7.4 Hz), 0.94 (t, 3H, CH_3, J = 7.4 Hz; ^{13}C NMR {H} (DMSO-d_6, 75 MHz): δ (ppm): 167.6 (C20), 162.9 (C17), 155.1 (C5), 152.1 (C6), 147.4 (C9), 130.0 (C8), 129.1 (C15, C19), 127.5 (C7), 115.7 (C16, C18), 115.5 (C14), 86.8 (C2), 68.1 (CH_2), 31.0 (CH_2), 21.4 (C22), 19.1 (CH_2), 14.9 (CH_3); Anal. Calcd for ($C_{18}H_{19}N_3O_5S$): C, 55.52; H, 4.96; N, 10.79. Found: C, 56.01; H, 3.51; N, 11.15.

4.1.4.13. 3-Acetyl-5-(4-nitrophenyl)-2-(5-nitrothiophen-2-yl)-2,3-dihydro-1,3,4-oxadiazole (5m). Yellow solid (57%); mp 186.0–187.0 °C. ^{1}H NMR (DMSO-d_6, 300 MHz): δ (ppm): 8.40 (d, 2H, H16/18, J = 9.0 Hz); 8.11 (d, 2H, H15/19, J = 9.0 Hz); 8.07 (d, 1H, H8, J = 4.6 Hz) 7.63 (s,1H, H2); 7.52 (d, H7, J = 4.3 Hz); 2.33 (3H, H22). ^{13}C NMR {H} (DMSO-d_6, 75 MHz): δ (ppm): 167.7 (C20), 153.0 (C5), 152.2 (C6), 149.4 (C9), 146.2 (C17), 129.3 (C14), 128.0 (C8), 127.2 (C7, C15, C19), 124.1 (C16, C18), 87.8 (C2), 21.0 (C22); Anal. Calcd for ($C_{14}H_{10}N_4O_6S$): C, 46.41; H, 2.78; N, 15.46. Found: C, 46.50; H, 2.76; N, 15.30.

4.1.4.14. 3-Acetyl-5-(4-cyanophenyl)-2-(5-nitrothiophen-2-yl)-2,3-dihydro-1,3,4-oxadiazole (5n). Yellow solid (53%); mp 136.0–137.0 °C. ^{1}H NMR (DMSO-d_6, 300 MHz): δ (ppm): 8.08 (d, 2H, H15/19, J = 4.2 Hz); 8.02 (s, 3H, H18/16 e H8); 7.62 (s, 1H, H2), 7.51 (d, H7, J = 4.2 Hz); 2.32 (3H, H22). ^{13}C NMR {H} (DMSO-d_6, 75 MHz): δ (ppm): 167.7 (C20), 157.3 (C5), 153.2 (C6), 152.0 (C9), 146.3 (C14), 133.0 (C16, C18), 129.5 (C8), 127.5 (C7), 127.3 (C15, C19), 118.0 (CN), 114.3 (C17), 87.6 (C2), 21.1 (C22). Anal. Calcd for ($C_{15}H_{10}N_4O_4S$): C, 52.63; H, 2.94; N, 16.37. Found: C, 49.76; H,3.78; N, 15.83.

4.1.4.15. 3-Acetyl-5-(4-acetoxyphenyl)-2-(5-nitrothiophen-2-yl)-2,3-dihydro-1,3,4-oxadiazole (5o). Yellow solid (75%); mp 120.0–121.0 °C. ^{1}H NMR (DMSO-d_6, 300 MHz): δ (ppm): 8.06 (d, 1H, H8, J = 4.3 Hz); 7.93 (d, 2H, H16/18, J = 8.6 Hz); 7.57 (s, 1H, H_2); 7.48 (d, H_7, J = 4.3 Hz); 7.35 (d, 2H, H15/19 J = 8.6 Hz); 2.32 (6H, H22 e $OCOCH_3$); ^{13}C NMR {H} (DMSO-d_6, 75 MHz): δ (ppm): 168.8 (C20), 167.4 (C=O), 154.0 (C5), 153.3 (C6), 151.7 (C17), 146.6 (C9), 129.4 (C14), 128.2 (C15, C19), 127.1 (C8), 122.8 (C16, C18), 120.8 (C7), 87.0 (C2), 21.0 (C22), 20.8 (CH_3). Anal. Calcd for ($C_{16}H_{13}N_3O_6S$): C, 51.20; H, 3.49; N, 11.19. Found: C, 51.10; H, 3.55; N, 11.06.

4.2. Biology

The biological activity of the nitrocompound derivatives was evaluated against the epimastigote form of *T. cruzi* Y strain, *S aureus* ATCC 25923, multidrug-resistant *S. aureus* 3SP/R33 and VISA3 strains, and *Candida albicans* ATCC537Y.

4.2.1. In vitro anti-*T. cruzi* activity

The parasite epimastigote form, at the stationary phase and from a culture incubated for 10 days at 28 °C, was diluted into liver infusion tryptose (LIT) medium to obtain a final concentration of 2.0×10^6 parasites per mL. The LIT medium was prepared as

described in a previous study.[13] A preliminary assay using the inocula at logarithmic phase was performed, indicating the derivative compounds that presented a good potential profile. The nitroderivatives and benznidazole (BZN), the standard drug, were separately dissolved in dimethylsulphoxide, DMSO, (Labsynth, São Paulo, Brazil) and diluted into LIT culture medium to obtain a concentration from 1.25 to 40.0 μM, depending on the solubility of the compounds. An aliquot of the inocula containing 2.0×10^6 viable parasites per mL[21,22] was added to the compounds being evaluated and incubated at 28 °C for 5 days. After this period, the amount of viable parasites was determined using a spectrophotometer (T80 plus, PG Instruments, United Kingdom) at 580 nm (10 mm light path length). The assays were performed in triplicate and the remaining parasites were counted in a Neubauer chamber. The anti-*T. cruzi* activity was determined by the relation.[23–28]

$$PGI = 1 - [(A_P - A_{0P})/(A_C - A_{0C})] \times 100,$$

where: PGI = percentage of growth inhibition; $A_p = A_{580}$ of the culture containing the drug at day 5; $A_{0p} = A_{580}$ of the culture containing the compound after the addition of the inoculums at day 0; $A_c = A_{580}$ of the culture in the absence of any compound at day 5; $A_{oc} = A_{580}$ of the culture in the absence of any compound at day 0.

4.2.1.1. IC_{50} determination. The inhibitory concentration 50%, IC_{50}, was calculated from the percentage of inhibition growth using a dose–response curve for each case, using at least four concentration values.

4.2.2. Antibacterial activity[20]

Minimal Inhibitory Concentration (MIC) of the compounds was determined with 96-well microtiter plates containing twofold serial dilutions of the compounds in Tryptic Soy Broth (TSB, Sigma-Aldrich®) medium. Stock solutions of the compounds were prepared in DMSO/TSB 1:10 v/v. Concentrations ranged from 0.1 to 80 μg/mL, using nifuroxazide, ampicilin, and vancomycin as drug controls. Bacterial suspensions were prepared by turbidity adjustment to a density of 0.5 on the McFarland scale and further dilution in sterile physiologic saline solution and TSB. The plates were incubated at 35 °C for 18 h, and the lowest concentration of compound at which there was no visible growth was considered as being the MIC value. Readings at 24 and 48 h were carried out for sterility control. All assays were performed in triplicate.

4.2.3. Antifungal activity

Antifungal susceptibility against *Candida albicans* ATCC537Y was performed according to CLSI document M27-A2.[29] Sensitivity was increased in a second phase assay, adapting the methodology described by Jorge et al.[20] Stock solutions of the compounds were prepared using RPMI 1640 (Sigma-Aldrich®) with 20% DMSO, in concentrations varying from 20 to 30 μg/mL depending on solubility. Serial dilutions were prepared in 96-well microtiter plates, the wells inoculated with a suspension of *C. albicans* into RPMI 1640 at final concentration equivalent of 10^3–10^5 CFU/mL, and the microplates incubated at 35 °C for 48 h. MIC was determined as being the lowest concentration where a proeminent reduction in growth was observed. DMSO at concentrations above 5% v/v had a growth inhibition effect on *C. albicans* and wells presenting those concentrations were disregarded when determining MIC values. The assays were performed in triplicate and fluconazole was used as standard drug.

4.3. Molecular modeling approach

The three-dimensional models of the 3-acetyl-2,5-disubstituted-2,3-dihydro-1,3,4-oxadiazole derivatives were constructed in their neutral forms using as starting geometry a derivative of 1,3,4-oxadiazole whose crystallographic information was retrieved from Ref. 30. Each model was energy-minimized in the MM+ force field[31] without any constrains (HyperChem 7.51[32]). The partial atomic charges were calculated employing the AM1 semiempirical method.[33] Molecular dynamics (MD) simulations [1 ns; size step 1 fs; 310 K] were carried out using the MOLSIM 3.2 program.[34] The lowest-energy conformer selected from MD simulation of each compound was the input structure for calculating the physicochemical and structural properties explored in this study. Electrostatic partial atomic charges (CHELPG)[35] were computed using the B3LYP/3-21G* method[36,37] implemented in the GAUSSIAN 03 W program.[38] The EP property was calculated in a cube surface using an isovalue of 0.0004 (GAUSSIAN 03 W).[38] Negative values of EP (higher electronic density) are denoted as intense red while positive values are mapped in blue (lower electronic density) on the molecular surfaces. The LP property was computed onto a Connolly molecular surface[39,40] employing a sphere probe of 1.4 Å radii (Sybyl 8.0 package[18]). This property and the *C* log *P* values were calculated applying the Ghose and co-workers method[16] and Sybyl Line Notation (SLN)[17] (Sybyl 8.0 package[18]). The resulting LP maps were evaluated regarding the color ramps, which range from dark brown (hydrophobic or lipophilic region on molecular surface) to blue (hydrophilic area on molecular surface). It is noteworthy that the color scheme is easy to interpret if the blue is associated with water and the brown as oil/fat. Furthermore, the atomic steric hindrance of each model was calculated from the covalent radii values and geometrical distances, using the Calculator Plugins at the Marvin 5.3.8 software.[19] This structural feature is additive, meaning that the total steric hindrance of a substituent group corresponds to the sum of each atomic steric hindrance calculated.[19]

Acknowledgments

The authors thank Professor Elza Masae Mamizuka, from the Department of Clinical and Toxicological Analysis, USP, for providing the 3SP/R33 and VISA3 *S. aureus* strains and Professor Maria Júlia Manso Alves, from Chemistry Institute for providing the epimastigote form of *T. cruzi* strain. The authors thank Brazilian scientific committees, CNPq and FAPESP for the financial support.

References and notes

1. Rice, L. B. *Am. J. Infect. Control* **2006**, *34*, S11.
2. Pfaller, M. A.; Pappas, P. G.; Wingard, J. R. *Clin. Infect. Dis.* **2006**, *43*, S3.
3. Urbina, J. A.; Docampo, R. *Trends Parasitol.* **2003**, *19*, 495.
4. Siles, R.; Chen, S.; Zhou, M.; Pinney, K. G.; Trawick, M. L. *Bioorg. Med. Chem. Lett.* **2006**, *16*, 4405.
5. Zhao, H.; Guo, Z. *Drug Discovery Today* **2009**, *14*, S16.
6. Masunari, A.; Tavares, L. C. *Br. J. Pharm. Sci.* **2006**, *42*, 461.
7. Behrouzi-Fardmoghadam, M.; Poorrajab, F.; Ardestani, S. K.; Emami, S.; Shafiee, A.; Foroumadi, A. *Bioorg. Med. Chem.* **2008**, *42*, 4509.
8. Rollas, S.; Gulerman, N.; Erdeniz, H. *Il Farmaco* **2002**, *57*, 171.
9. Parmar, S. S.; Gupta, A. K.; Gupta, T. K.; Stenberg, V. I. *J. Pharm. Sci.* **1975**, *64*, 154.
10. Kalsi, R.; Pande, K.; Balla, T. N.; Bartwall, J. P.; Gupta, G. P.; Parmar, S. S. *J. Pharm. Sci.* **1990**, *79*, 317.
11. Li, C.; Ma, Y.; Cao, L. *J. Chin. Chem. Soc.* **2009**, *56*, 182.
12. Masunari, A.; Sonehara, I. Y.; Pasqualoto, K. F. M.; Tavares, L. C. *QSAR Comb. Sci.* **2009**, *28*, 1546.
13. Paula, F. R.; Jorge, S. D.; Almeida, L. V.; Pasqualoto, K. F. M.; Tavares, L. C. *Bioorg. Med. Chem.* **2009**, *17*, 2673.
14. Masunari, A.; Tavares, L. C. *Bioorg. Med. Chem.* **2007**, *15*, 4229.
15. Cao, C.; Liu, L. *J. Chem. Inf. Comput. Sci.* **2004**, *44*, 678.
16. Ghose, A. K.; Viswanadhan, V. N. J.; Wendoloski, J. *J. Phys. Chem. A* **1998**, *102*, 3762.
17. Ash, S.; Cline, M. A.; Homer, R. W.; Hurst, T.; Smith, G. B. *J. Chem. Inf. Comput. Sci.* **1997**, *37*, 71.
18. Sybyl 8.0 for Linux; Tripos, Inc.: 2007. 1699 South Hanley Rd., St. Louis, MO 63144-2917, USA.
19. Marvin 5.3.8 software – Calculator Plugins, 2010, ChemAxon Ltd., Budapest, 1037, Hungary (http://www.chemaxon.com).

20. Jorge, S. D.; Masunari, A.; Rangel-Yagui, C. O.; Pasqualoto, K. F. M.; Tavares, L. C. *Bioorg. Med. Chem.* **2009**, *17*, 3028.
21. Schvartzapel, A. J.; Zhong, L.; Docampo, R.; Rodriguez, J. B.; Gros, E. G. *J. Med. Chem.* **1997**, *40*, 2314.
22. Elhalem, E.; Bailey, B. N.; Docampo, R.; Ujváry, I.; Szajnman, S. H.; Rodriguez, J. B. *J. Med. Chem.* **2002**, *45*, 3984.
23. Cerecetto, H.; Maio, R. D.; Ibarruri, G.; Seoane, G.; Denicola, A.; Pefullo, G.; Quijano, C.; Paulino, M. *Il Farmaco* **1998**, *53*, 89.
24. Aguirre, G.; Boiani, L.; Boiani, M.; Cerecetto, H.; Di Maio, R.; González, M.; Porcal, W.; Denicola, A.; Piro, O. E.; Castellano, E. E.; Sant'anna, C. M. R.; Barreiro, E. J. *Bioorg. Med. Chem.* **2005**, *13*, 6336.
25. Arán, V. J.; Ochoa, C.; Boiani, L.; Buccino, P.; Cerecetto, H.; Gerpe, A.; González, M.; Montero, D.; Nogal, J. J.; Gomez-Barrio, A.; Azqueta, A.; Cerain, A. L.; Piro, O. E.; Castellano, E. E. *Bioorg. Med. Chem.* **2005**, *13*, 3197.
26. Cerecetto, H.; Di Maio, R.; Risso, M.; Saenz, P.; Seoane, G.; Denicola, A.; Peluffo, G.; Quijano, C.; Olea-Azar, C. *J. Med. Chem.* **1999**, *42*, 1941.
27. Aguirre, G.; Cerecetto, H.; Di Maio, R.; González, M.; Porcal, W.; Seoane, G.; Ortega, M. A.; Aldana, I.; Monge, A.; Denicola, A. *Arch. Pharm.* **2002**, *335*, 15.
28. Aguirre, G.; Boiani, L.; Cerecetto, H.; Di Maio, R.; González, M.; Porcal, W.; Denicola, A.; Moller, M.; Thomson, L.; Tortora, V. *Bioorg. Med. Chem.* **2005**, *13*, 6324.
29. National Committee for Clinical Laboratory Standards. Reference Method for Broth Dilution Antifungal Susceptibility Testing of Yeasts. Approved Standards. Document M27A2. Wayne, PA: National Committee for Clinical Laboratory Standards, 2002.
30. Wang, X.; Wang, W.; Liu, H. X. *Acta Crystallogr., Sect. C* **1995**, *51*, 1585.
31. Allinger, N. L. *J. Am. Chem. Soc.* **1977**, *99*, 8127.
32. HyperChem Program Release 7.51 for Windows; Hypercube, Inc., Gainesville, FL 2002.
33. Dewar, M. J. S. E.; Zoebisch, G.; Healy, E. F.; Stewart, J. J. P. *J. Am. Chem. Soc.* **1985**, *107*, 3902.
34. Doherty, D. MOLSIM: Molecular Mechanics and Dynamics Simulation Software, version 3.2 – User's Guide. The Chem21 Group Inc., 1780 Wilson Dr., Lake Forest, IL, 60045, EUA, 2002.
35. Breneman, C. M.; Wiberg, K. B. *J. Comput. Chem.* **1990**, *11*, 361.
36. Becke, A. D. *Phys. Rev. A* **1988**, *38*, 3098.
37. Lee, C.; Yang, W.; Parr, R. G. *Phys. Rev. B* **1988**, *37*, 785.
38. Gaussian 03, Revision B.03, Frisch, M. J.; Trucks, G. W.; Schlegel, H. B.; Scuseria, G. E.; Robb, M. A.; Cheeseman, J. R.; Montgomery, J. A.; Jr., Vreven, T.; Kudin, K. N.; Burant, J. C.; Millam, J. M.; Iyengar, S. S.; Tomasi, J.; Barone, V.; Mennucci, B.; Cossi, M.; Scalmani, G.; Rega, N.; Petersson, G. A.; Nakatsuji, H.; Hada, M.; Ehara, M.; Toyota, K.; Fqytqterukuda, R.; Hasegawa, J.; Ishida, M.; Nakajima, T.; Honda, Y.; Kitao, O.; Nakai, H.; Klene, M.; Li, X.; Knox, J. E.; Hratchian, H. P.; Cross, J. B.; Adamo, C.; Jaramillo, J.; Gomperts, R.; Stratmann, R. E.; Yazyev, O.; Austin, A. J.; Cammi, R.; Pomelli, C.; Ochterski, J. W.; Ayala, P. Y.; Morokuma, K.; Voth, G. A.; Salvador, P.; Dannenberg, J. J.; Zakrzewski, V. G.; Dapprich, S.; Daniels, A. D.; Strain, M. C.; Farkas, O.; Malick, D. K.; Rabuck, A. D.; Raghavachari, K.; Foresman, J. B.; Ortiz, J. V.; Cui, Q.; Baboul, A. G.; Clifford, S.; Cioslowski, J.; Stefanov, B. B.; Liu, G.; Liashenko, A.; Piskorz, P.; Komaromi, I.; Martin, R. L.; Fox, D. J.; Keith, T.; Al-Laham, M. A.; Peng, C. Y.; Nanayakkara, A.; Challacombe, M.; Gill, P. M. W.; Johnson, B.; Chen, W.; Wong, M. W.; Gonzalez, C.; Pople, J. A. Gaussian, Inc., Pittsburgh PA, 2003.
39. Connolly, M. L. *Science* **1983**, *221*, 709.
40. Connolly, M. L. *J. Appl. Crystallogr.* **1983**, *16*, 548.